Phase Characterization of Reflectarray Elements at Infrared

James C. Ginn, *Student Member, IEEE*, Brian A. Lail, *Senior Member, IEEE*, and Glenn D. Boreman, *Senior Member, IEEE*

***Abstract*—The feasibility of a square-patch reflectarray element design is demonstrated at a frequency of 28.3 THz in the infrared (10.6 micrometer free-space wavelength) for the first time. Fabrication of arrays of various patch sizes was performed using electron-beam lithography, and the reflected phase as a function of patch size was characterized using an infrared interferometer. A numerical model for the design of these reflectarray elements was developed incorporating measured values of frequency-dependent material properties, and a comparison of computed and measured phase shows close agreement.**

***Index Terms*—Infrared, microstrip reflectarray.**

I. Introduction

REFLECTARRAYS are traditionally passive, planar microstrip antenna arrays designed for discrete reflected phase manipulation at each individual antenna element making up the array. By spatially varying the phase response of the antenna array, reflectarrays allow a planar surface to impress a non-planar phasefront on the reflected radiation, for example, a spherical wavefront. Initially proposed as a low-cost replacement for mechanically bulky parabolic reflectors, reflectarrays have been successfully developed and utilized at both radio (RF) [1] and millimeter-wave (mmW) [2] frequencies.

While reflectarray technology has rapidly matured at RF and mmW, there have been no demonstrations to date of reflectarray feasibility in the infrared (IR). In principle, existing reflectarray technologies can simply be scaled for use at these higher frequencies; however, a straightforward frequency translation is complicated by complex frequency-dependent material properties, as well as limitations in fabrication and testing. For verification of the proposed design procedures, several IR reflectarray proof-of-concept devices operating at 28.3 THz have been modeled, fabricated and characterized.

Infrared reflectarrays are desirable for many of the reasons they are desirable for use at lower frequencies, such as reduced cost, weight, and volume for focusing surfaces. Reflectarrays facilitate direct stacking of multiple planar elements, (e.g., filters and polarizers) on the reflectarray for additional weight and volume reductions. It may also be that IR reflectarrays will be seen to provide additional degrees of freedom not previously available in conventional polished and diffractive IR-optical surfaces for correction of monochromatic and chromatic aberrations.

Manuscript received August 1, 2006; revised May 31, 2007. This work was supported in part by the Lockheed Martin Corporation under Grant and in part by the Florida High Tech Corridor Council.

J. C. Ginn and G. D. Boreman are with the CREOL/College of Optics and Photonics, University of Central Florida, Orlando, FL 32816 USA (e-mail: jcginn@creaol.ucf.edu).

B. A. Lail is with the Department of Electrical and Computer Engineering, Florida Institute of Technology, Melbourne, FL 32901 USA.

Digital Object Identifier 10.1109/TAP.2007.908537

II. Reflectarray Proof-of-Concept Design

Perhaps the main issue that differentiates IR reflectarray element designs from their RF counterparts is the need to account for frequency-dependent complex material properties. In the IR, dielectric loss and dispersion are important considerations for candidate standoff-layer materials, and must be included for an accurate design. Metals in this frequency range also have significant frequency-dependent losses as well as skin-depth variations with frequency. As a first step in the modeling, it is reasonable to include curve-fitted values of permittivity or conductivity from a simple dispersion relation (e.g., Drude model, [3]) or from previously published data measured for bulk materials. However, variations in deposition techniques, layer thickness, atmospheric conditions, material composition, and handling can introduce significant variations in the material properties, and it is desirable for accurate modeling to include properties of the as-deposited materials and films, measured at the frequencies of interest. For this purpose, we use a commercial infrared variable-angle spectroscopic ellipsometer (IR-VASE), which allows measurement of real and imaginary refractive index over the wavelength range from 3 to 30 μm. Measured material data are thus imported into our computational models at each frequency of interest [4].

Based on measured ellipsometric data, zirconium dioxide (ZrO_2) was chosen as the reflectarray standoff material because of its low values of loss tangent and relative permittivity at 10.6 μm [see Fig. 1(a)], which tend to improve the power efficiency of the resulting reflectarray. To reduce metallic losses, Gold (Au) was used for both the reflectarray ground plane and patch elements because of its relatively high conductivity at infrared frequencies [see Fig. 1(b)] and its low chemical reactivity at room temperature. A patch thickness of 150 nm, approximately 15 times the skin depth of Au at 10.6 μm, was used to reduce unwanted skin-depth effects. Patch element spacing was chosen to be 5.54 μm, approximately 60% the effective wavelength at 10.6 μm. For the stand-off layer, a ZrO_2 thickness of 450 nm satisfied isolation conditions and limited the dielectric losses.

The reflectarray element geometry was selected to ease fabrication tolerances, which are typically stringent in the IR. A variable-patch reflectarray [5]–[9] element was chosen since it was previously demonstrated at RF to have numerous advantages [10] desirable for deployment at higher frequencies. Unlike ring-element designs, the square patch reflectarray is

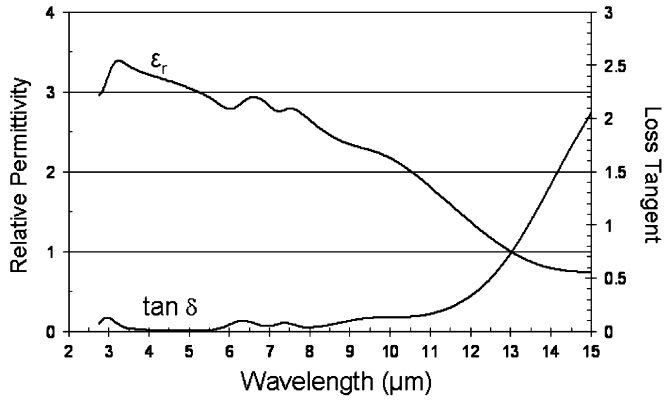

(a)

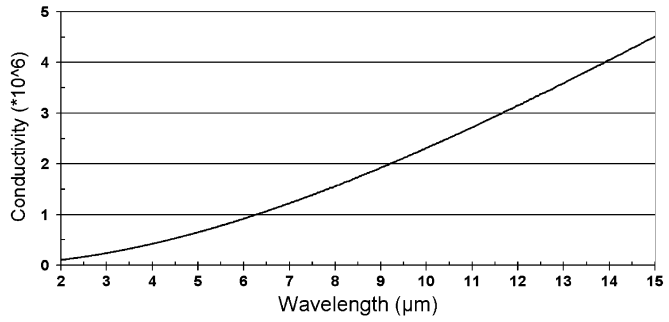

(b)

Fig. 1. Measured dielectric properties for (a) ZrO_2. (b) Measured conductivity properties for Au.

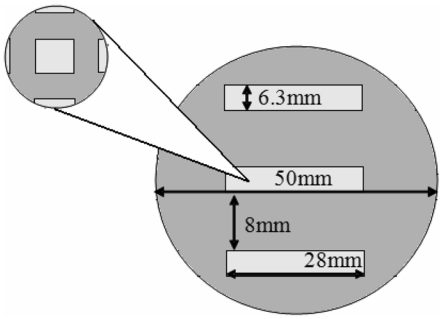

Fig. 2. IR reflectarray proof-of-concept layout.

easily fabricated with a high degree of accuracy. Patch sizes scale well with frequency as opposed to reflectarray elements that utilize stubs to generate phase delays. Most significantly, variable-patch reflectarrays demonstrate superior bandwidths when compared to other non-broadband elements and have been demonstrated to reach bandwidths of 15% in specific configurations [11]. The bandwidth of the reflectarray will be important when extending the functionality of the designs to cover a wider range in the IR, such as the 8- to 12-μm wavelength band.

The purpose of the design was to characterize the phase response as a function of element design for a given choice of materials, as a preliminary proof-of-concept demonstration prior to proceeding to more complex designs, such as a focusing array. Thus, a simple 50-mm diameter substrate, three-stripe reflectarray prototype configuration was developed (Fig. 2)

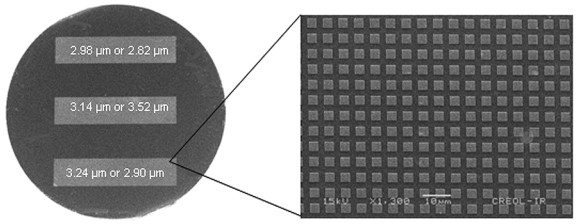

Fig. 3. Visible image of IR reflectarray and SEM image of one patch stripe.

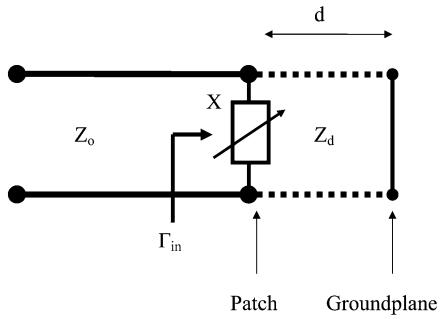

Fig. 4. Reflectarray transmission line equivalent.

especially suited for interferometric characterization. The three reflectarray stripes are 6.3-mm by 28-mm rectangular arrays of square patches of uniform size, isolated from each other by 8-mm blank reference regions. The array comprising each stripe was made up of a single-sized patch element to demonstrate a unique phase shift upon reflection for comparison between the modeled and measured results. To ensure that any phase shift on reflection was caused by the reflectarray and not the substrate, a 3-mm thick, fused-silica optical flat (peak-to-valley flatness variation less than 160 nm) was chosen as the mechanical support substrate for the reflectarrays.

For investigation of reflectarray element behavior at IR, three multiple-stripe arrays were fabricated for testing at 10.6 μm. The first array (array #1) used the patch dimensions of 2.98 μm, 3.14 μm, and 3.24 μm and the second array (array #2) was fabricated with patches of size 2.82–, 2.9-, and 3.52-μm. Finally, a third array (array #3) was fabricated using a slightly modified layout to accommodate a larger number of stripes with patch sizes of 3.3-, 3.4-, 3.7-, 3.9-, and 4.1-μm. Images of array #1 and one of the reflectarray stripes are presented in Fig. 3.

III. Modeling

A. Reflectarray Transmission Line Equivalent

A practical approach to understanding ideal reflectarray element behavior, for the purpose of initial design validation at RF, has been to relate the structure to a lossless circuit equivalent [12], [13]. Variable-patch reflectarrays achieve phase shift modification upon reflection through variation of element size and, thus, the resonant frequency of the square microstrip patch. A slight variation in the resonant frequency of the scattering patch modulates the phase of the standing wave formed between the patch and the groundplane, which in turn alters the phase of the re-radiated wave. Scattering patches can be represented as a terminated transmission line (Fig. 4). Beginning at the termination,

the reflectarray groundplane will behave as a short, exhibiting a reflection coefficient of -1 corresponding to the expected 180° phase shift upon reflection by a plane wave impinging on a perfect electric conductor (PEC) surface. The stand-off layer of the reflectarray can be modeled as the transmission line with characteristic impedance equal to the wave impedance of the stand-off layer material (Z_d) and with length equal to the height of the stand-off layer (d). Assuming the width and length of the patch are equal, the patch itself can be represented as a purely reactive element, with reactance (X) dependent on the ratio of the area of the symmetric patch (l^2) relative to the area of the unit cell (A). Thus, when the area of the patch approaches zero, the element will behave as an open, and when the area of the patch approaches the area of the unit cell the inductor will behave as a short. The unit cell is finally connected to the open terminals of an infinite waveguide with characteristic impedance (Z_o) equal to the free-space wave impedance.

Determination of the phase shift can be directly calculated by finding the input reflection coefficient at the interface between the stand-off layer transmission line and the air transmission line. Using conventional transmission line calculations, the reflection coefficient $(\Gamma_{\rm in})$ is represented by

$$\Gamma_{\rm in} = \frac{Z_{\rm in} - Z_0}{Z_{\rm in} + Z_0} \tag{1}$$

where the input impedance $(\mathrm{Z_{in}})$ can be found by adding, in parallel, the impedance of the patch and the impedance of the transmission line referred to the interface location. This yields

$$Z_{\rm in} = \left[\frac{1}{X(l^2, A)} + \frac{-j\cot\left[\frac{2\pi\sqrt{\varepsilon_r}d}{\lambda_0}\right]}{Z_d} \right]^{-1} \tag{2}$$

where λ_0 is the free space wavelength and $\varepsilon_{\rm r}$ is the real part of the stand-off layer's dielectric constant. Finally the phase response of the reflectarray can be calculated by finding the phase of $\Gamma_{\rm in}$.

As seen from the calculations, the height of the standoff layer determines the extent of the phase shift achievable by the reflectarray. In the situation where the patch area is small enough not to introduce any significant reactance, the reflectarray phase response is simply determined by the roundtrip propagation through the standoff layer, including the phase shift from the ground plane reflection. When the patch approaches the size of the unit cell, it will begin to behave as a short, independent of the stand-off layer and groundplane. Thus, the shortest possible standoff-layer height should be used that achieves nearly 360° of phase shift at the design frequency, in order to minimize any dielectric loss. Between the large-patch and small-patch limits, the input impedance is dependent on the area of the patch, which will result in a non-linear relationship between the phase response of the patch and the length of the patch due to the Kramers–Kronig relationship between the phase and reflectivity response of the element at and around the resonance of design.

B. Numerical Modeling

Although useful for a conceptual understanding of a variable patch reflectarray element at infrared, lossless circuit equivalents are limited in accuracy and the next step in the design process, even at RF, is to employ some form of a computational electromagnetic modeler (CEM) [14]. Numerical modeling takes into account system non-idealities, such as lossy materials or mutual coupling, which are difficult to incorporate into simplified circuit or transmission line element equivalent without a significant increase in complexity. In addition, accurate circuit models are problematic for infrared designs given material dispersion and the significant dependence of a patch's resonant Q on metal conductivity. Although coupling between patches shorted to a groundplane is relatively low [15], coupling has been demonstrated to have a significant impact on reflectarray performance [16] and should be accounted for in models, rather than simply using a single element or a waveguide modeling approach. Thus, for modeling, Ansoft's commercially available method of moments CEM, Designer, was employed for characterizing the reflectarray elements. In Designer, coupling is accounted for by using a fictional periodic boundary. The periodic boundary suppresses edge currents arising from the modeling of a single element by a solution of the periodic Green's function in the bound two dimensional space [17]. Model excitation is achieved by a linearly polarized plane wave at normal incidence. Finally, for the highest degree of accuracy in modeling, it was necessary to include measured optical properties in the model. Designer does not currently support dispersive materials and our computations required an external software program [4] for importing measured IR-material data.

IV. Fabrication

Fabrication began by depositing a 200-nm Au ground plane on a 50-mm optical flat, with a 10-nm titanium (Ti) adhesion layer on the top and bottom of the gold layer, followed by an ion-assisted e-beam evaporation deposition of the 450 nm layer of ZrO_2. The exposed face of the ZrO_2 was then cleaned in preparation for writing and a bi-layer of commercially available electron beam resist was spun on consisting of 400 nm of a Polymethylglutarimide (PMGI) SF7 resist under layer and a 300 nm top layer of ZEP 520-A7 high resolution positive resist. A resist bi-layer was deemed necessary to insure that no deposited patches were accidentally removed or damaged during the resist lift-off process. The resist-coated wafer was then loaded into the holder, held in place by the two clips, and loaded into the Leica EBPG5000+ for vacuum pump down. Pattern exposure for the reflectarray lasted for approximately 2.5 h, upon which the exposed wafer was removed from the chamber, ready for development.

Development of the resist bi-layer was a two-step process. The exposed ZEP layer was developed and removed by first putting the wafer in ZEP RD developer. After that, the exposed PMGI under layer was developed by using MF 701 developer to fully develop the patch stripe pattern. The developed wafer was then loaded into an e-beam evaporator. Similar to deposition process used in depositing the groundplane, a 150-nm Au layer, with a Ti adhesion layer, was evaporated onto the wafer. A final lift-off process was employed to remove the unwanted metal and undeveloped resist. The ZEP layer was then lifted-off in a methylene chloride ultrasound bath and the remaining PMGI layer was removed using EBR PG remover in ultrasound.

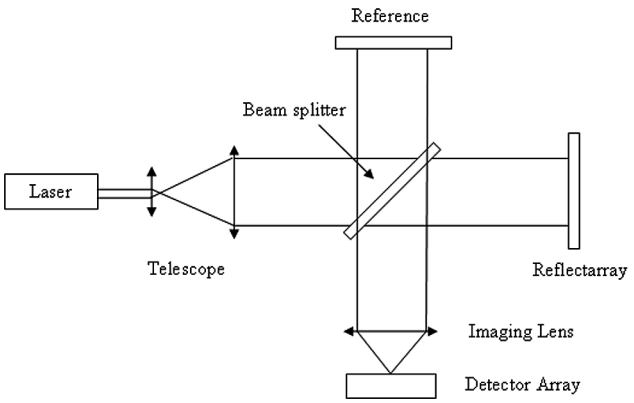

Fig. 5. Twyman-Green interferometer.

V. Testing and Results

The phase shift on reflection of the reflectarray stripes, compared to that of the adjacent reference regions between the stripes was measured at 28.3 THz (10.6-μm free-space wavelength) using a commercially available Twyman-Green interferometer [18], the Wyko IR3. For a typical Twyman–Green interferometer (Fig. 5), a beam from a coherent light source (a 10.6 μm CO_2 Synrad laser for the IR3) is initially expanded and collimated with a two lens telescope, to achieve near plane wave excitation. The source was also linearly polarized along the largest dimension of the reflectarray stripes. The collimated beam impinges on a beam splitter where half of the beam will reflect off of the test device back into the interferometer and the other half of the beam will reflect off of a flat reference surface inside the interferometer, typically a gold mirror for tilt adjustment and correction. The two beams are then recombined in the beamsplitter and focused to an array of IR detectors for imaging of the generated interference pattern arising from the test and the reference beams. If the reference has a slight tilt relative to the device, a series of straight interference fringes will be present, corresponding to the spatial path length differences arising because of the tilt of the reference mirror. Thus, departures from straightness of the interference fringes are indicative of local variation of the phase shift on reflection at the device. Typically, for polished optics, these variations are caused by local height variations on the surface being characterized. However, for the physically flat reflectarray, the fringe deviations were a direct measurement of the phase shift produced entirely by the array elements.

Measured interferogram results for are seen in Fig. 6, for the fused-silica substrate without a reflectarray, array #1, and array #2, respectively. It can be seen that the bare substrate is essentially flat at 10.6 μm, verifying that fringe deviations seen in Fig. 6(b) and (c) are caused by the reflectarray patches. To determine the actual phase shift at each stripe, it is possible to spatially measure the fringe displacement at each reflectarray stripe relative to the nearest blank regions. It should be noted that the distance between the fringes represents a phase shift of 180° due to the single-pass nature of the reflectarray elements. A MATLAB function was developed to follow the fringe patterns captured by the interferometer and to compute the relative phase response, while automatically accounting for

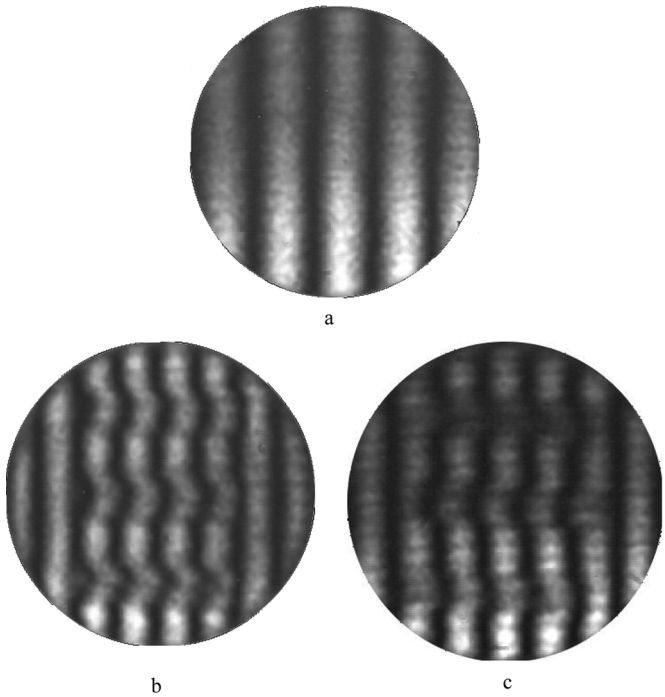

Fig. 6. Interferograms of reference flat and both fabricated reflectarrays. (a) Bare substrate. (b) Array #1. (c) Array #2.

TABLE I
Measured Phase Response of Fabricated Reflectarrays

Patch Size	Relative Phase Shift Upon Reflection
2.82 μm	174.4 °
2.90 μm	172.4 °
2.98 μm	136.4 °
3.14 μm	124.1 °
3.24 μm	110.3 °
3.3 μm	79.7 °
3.4 μm	56.3 °
3.52 μm	-56.2 °
3.70 μm	-95.1 °
3.90 μm	-109.3 °
4.10 μm	-112.4 °

the height difference between the patch rows and the groundplane. Reflectivity measurements were also taken of each reflectarray stripe. Although the devices tested were relatively lossy, at around 50%–60% power reflectivity, future designs will likely employ alternative geometries and materials for improved reflectivity. Measured phase responses from all three prototypes are presented in Table I.

Comparing measured and modeled results from Ansoft Designer (Fig. 7) clearly demonstrates that reflectarray behavior is feasible at IR with unique phase shifts measured across the reflectarray stripes. The results show that fringe shifting occurs entirely due to the difference in size of the patches and not because of any physical height difference such as used in conventional polished optics or reflector antennas. The measured phase response of each of the stripes corresponds well with modeled results and a maximum phase shift of approximately 292.4° was measured. Additionally, the modeled results suggest that the present reflectarray geometry is not significantly impacted by metallic skin effects, when measured conductivity is utilized in the model. Most importantly, the results demonstrate the practicality of the proposed reflectarray element design procedures to

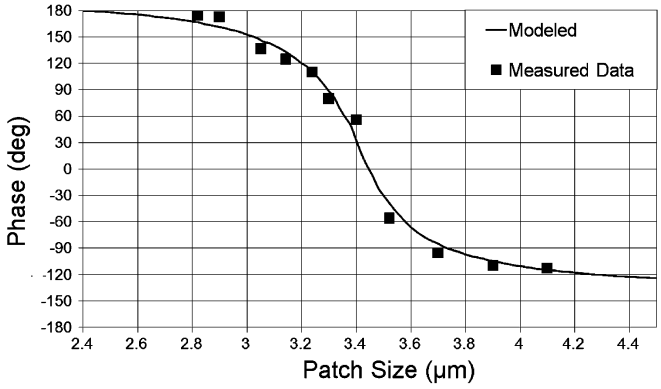

Fig. 7. Comparison of measured and modeled results.

accurately predict and characterize reflectarray behavior at infrared frequencies.

VI. Conclusion

The feasibility of a square-patch reflectarray element design was demonstrated at the infrared frequency of 28.3 THz. Fabrication of arrays of various patch sizes was performed using electron-beam lithography, and the reflected phase as a function of patch size was characterized using an infrared interferometer. The numerical model used for the design of these reflectarrays incorporated measured values of frequency-dependent material properties, and comparison of computed and measured phase demonstrates that the phase response is a function of patch dimensions.

Acknowledgment

The authors would like to thank G. Zummo for his support during fabrication and D. Zinn for access to the interferometer.

References

[1] D. Berry, R. Malech, and W. Kennedy, "The reflectarray antenna," *IEEE Trans. Antennas Propag.*, vol. 11, no. 6, pp. 645–651, Nov. 1963.

[2] D. M. Pozar, S. D. Targonski, and H. D. Syrigos, "Design of millimeter wave microstrip reflectarrays," *IEEE Trans. Antennas Propag.*, vol. 45, no. 2, pp. 287–296, Feb. 1997.

[3] E. Topsakal and J. Volakis, "On the properties of materials for designing filters at optical frequencies," in *Proc. IEEE Antennas and Propagation Society Int. Symp.*, Jun. 22–27, 2003, vol. 4, pp. 635–638.

[4] J. Ginn, B. Lail, D. Shelton, J. Tharp, W. Folks, and G. Boreman, "Characterizing infrared frequency selective surfaces on dispersive media," *ACES J.*, vol. 22, no. 1, pp. 184–188, Mar. 2007.

[5] D. Pozar and T. Metzler, "Analysis of a reflectarray antenna using microstrip patches of variable size," *Electron. Lett.*, vol. 29, no. 8, pp. 657–658, Apr. 15, 1993.

[6] F. Tsai and M. Bialkowski, "Designing a 161-element Ku-band microstrip reflectarray of variable size patches using an equivalent unit cell waveguide approach," *IEEE Trans. Antennas Propag.*, vol. 51, no. 10, pt. 2, pp. 2953–2962, Oct. 2003.

[7] D. Chang and M. Huang, "Multiple-polarization microstrip reflectarray antenna with high efficiency and low cross-polarization," *IEEE Trans. Antennas Propag.*, vol. 43, no. 8, pp. 829–834, Aug. 1995.

[8] F. Venneri, G. Angiulli, and G. Di Massa, "Design of microstrip reflect array using data from isolated patch analysis," *Microw. Opt. Technol. Lett.*, vol. 32, no. 6, pp. 411–414, 2002.

[9] J. Encinar, "Design of two-layer printed reflectarrays using patches of variable size," *IEEE Trans. Antennas Propag.*, vol. 49, no. 10, pp. 1403–1410, Oct. 2001.

[10] D. Pozar and S. Targonski, "A microstrip reflectarray using crossed dipoles," in *Proc. IEEE Antennas and Propagation Society Int. Symp.*, Jun. 21–26, 1998, vol. 2, pp. 1008–1011.

[11] J. Huang, "Bandwidth study of microstrip reflectarray and a novel phased reflectarray concept," in *Proc. IEEE Antennas and Propagation Society Int. Symp.*, Jun. 1995, pp. 582–585.

[12] M. R. Chaharmir, J. Shaker, M. Cuhaci, and A. Ittipiboon, "A broadband reflectarray antenna with double square rings," *Microw. Opt. Tech. Lett.*, vol. 48, no. 7, Jul. 2006.

[13] M. Bozzi, S. Germani, and L. Perregrini, "A figure of merit for losses in printed reflectarray elements," *IEEE Antennas Wireless Propag. Lett.*, vol. 3, pp. 257–260, 2004.

[14] N. Lenin and P. Rao, "Evaluation of the reflected phase of a patch using waveguide simulator for reflectarray design," *Microw. Opt. Technol. Lett.*, vol. 45, no. 6, pp. 528–531, 2005.

[15] R. Jedlicka, M. Poe, and K. Carver, "Measured mutual coupling between microstrip antennas," *IEEE Trans. Antennas Propag.*, vol. 29, no. 1, pp. 147–149, Jan. 1981.

[16] M. A. Milon, R. Gillard, D. Cadoret, and H. Legay, "Comparison between the 'infinite array' approach and the 'surrounded-element' approach for the simulation of reflectarray antennas," presented at the IEEE Antennas and Propagation Society Int. Symp., Albuquerque, NM, Jul. 9–14, 2006.

[17] Ansoft Designer Reference Manual Ansoft Corporation, 2004, Rel. 2.1.

[18] D. Malacara, *Optical Shop Testing*. New York: Wiley, Jan. 1992.

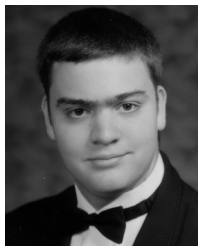

James C. Ginn (S'04) received the B.S. and M.S. degrees in electrical engineering from the University of Central Florida, Orlando, in 2004 and 2006 respectively, where he is currently working toward the Ph.D. degree in electrical engineering.

Since 2005, he has been a member of the Infrared Systems Laboratory research group at the CREOL/College of Optics and Photonics. His current research interests include infrared FSS and reflectarray design and high frequency computational electromagnetics.

Brian A. Lail (S'94–M'02–SM'07) received the B.S. degree in physics from Furman University, Greenville, SC, and the M.S. degree in physics from New Mexico State University, Las Cruces, in 1991 and 1994, respectively, and the M.S and Ph.D. degrees in electrical engineering from New Mexico State University, Las Cruces, in 1998 and 2002, respectively.

From 2002 to 2005, he was with the Department of Electrical and Computer Engineering at the University of Central Florida, Orlando. Since 2005, he has been an Assistant Professor in the Department of Electrical and Computer Engineering at Florida Institute of Technology, Melbourne, teaching and conducting research in applied and computational electromagnetics.

Glenn D. Boreman (S'80–M'84–SM'05) received the B.S. degree in optics from the University of Rochester, Rochester, NY, in 1978 and the Ph.D. degree in optical sciences from the University of Arizona, Tucson, in 1984.

Since 1984, he has been on the faculty of the University of Central Florida in Orlando, where he is currently Trustee Chair Professor of Optics, Physics, and Electrical Engineering. He is coauthor of *Infrared Detectors and Systems* (New York: Wiley, 1996) and the author of *Basic Electro-Optics for Electrical Engineers* (Bellingham, WA: SPIE, 1998) and *Modulation Transfer Function in Optical and Electro-Optical Systems* (Bellingham, WA: SPIE, 2001). His research interests include infrared and millimeter-wave sensing, and the transition of radiofrequency concepts such as antennas and frequency-selective surfaces to optical frequencies using electron-beam lithography.

Prof. Boreman is a Fellow of the Optical Society of America (OSA) and of the Society of Photo-Optical Instrumentation Engineers (SPIE). He served six years as Editor-in-Chief of OSA's journal *Applied Optics*, and is a past member of the SPIE Board of Directors. Along with his students, he received the 1995 Kingslake Medal from SPIE.